



Microscopy and phylogeny of *Pyramimonas tatianae* sp. nov. (Pyramimonadales, Chlorophyta), a scaly quadriflagellate from Golden Horn Bay (eastern Russia) and formal description of Pyramimonadophyceae classis nova

Niels Daugbjerg , Nicolai M.D. Fassel and Øjvind Moestrup 

Marine Biological Section, Dept of Biology, University of Copenhagen, Universitetsparken 4, 2100 Copenhagen Ø, Denmark

ABSTRACT

Nearly two decades ago a scaly quadriflagellate culture was established from a sample collected in Golden Horn Bay, eastern Russia. Here we present a comparative analysis of pheno- and genotypic characters and show that the isolate did not match any existing species of *Pyramimonas* and is therefore described as *P. tatianae* sp. nov. The species was probably identified as *P. aff. cordata* in previous studies on material from the same area. Based on an ultrastructural account of the cell and its external body scales it was found to belong to the subgenus *Vestigifera*. This was supported by a phylogenetic analysis using the chloroplast-encoded *rbcl* gene. The cell dimensions of *P. tatianae* were 6–7 µm long and 5–6 µm wide and it thus represented one of the smaller species of the genus. The cup-shaped chloroplast was divided into four lobes reaching from the middle to the anterior part of the cell. A single posterior eyespot was observed adjacent to an excentric pyrenoid. The ultrastructure of the body and flagellar scales were illustrated from material prepared for whole mounts and thin sections. The new species was compared with *P. cordata* and *P. mitra*, two other vestigiferans with which it shares some morphological features. The sequence divergence between *P. tatianae* and the most closely related species, *P. mitra*, was 2.5%. The phylogeny of *Vestigifera* revealed two lineages, one comprising cold-water species and the cosmopolitan *P. orientalis*, and the other species from temperate-subtropical waters. The tree topology suggested a southbound dispersal route. This was further supported by all antarctic *Pyramimonas* species having encystment stages as part of their life cycle. It was therefore probable that their ancestors also were capable of producing cysts allowing transportation over great distances. A formal description of the class Pyramimonadophyceae comprising both extant and extinct species was also provided.

ARTICLE HISTORY (Received 8 April 2019; Revised 4 June 2019; Accepted 14 June 2019)

KEY WORDS Dispersal; nanoflagellate; phylogeny; *Pyramimonas*; Pyramimonadophyceae; ultrastructure; *Vestigifera*

Introduction

Nearly 50 species of *Pyramimonas* have been described since Schmarda (1850) erected the genus with *P. tetra-rhynchus* as the type species. With the transfer of many species to *Hafniomonas* Ettl & Moestrup (Volvocales, Ettl & Moestrup, 1980), *P. tetra-rhynchus* is one of the very few freshwater species left in the genus. The oldest species descriptions were often short and accompanied by a few drawings, making identification of particularly the small round to ellipsoid species a challenging task (e.g. *P. delicatula* B.M. Griffiths (Griffiths, 1909); *P. inconstans* Hodgetts (Hodgetts, 1920)). With the introduction of the transmission electron microscope, identification, and thus, the taxonomy of these scaly green flagellates became less problematic as the morphology of body and flagellar scales proved to be suitable for species delineation. *Pyramimonas* has become one of the most species-rich genera among the scaly green flagellates and just over half of the total number of species were described during a 20-year period from 1980–1999 (Supplementary fig. S1). Species of

Pyramimonas reside in all major oceans and a few have, on rare occasions, been noted to form blooms (e.g. Inouye *et al.*, 1985; Thomsen, 1988; Gradinger, 1993; Tragin & Vaultot, 2018; Tragin *et al.*, 2018).

Based on a series of papers comparing the morphology of a diverse assemblage of species, the genus *Pyramimonas* was divided into six subgenera (McFadden *et al.*, 1986, 1987; Hori *et al.*, 1995). The main characters used for this subdivision included presence or absence of trichocysts, footprint scales, a curved synistosome and rows of puncta. Furthermore, the type of pyrenoid, underlayer and large body scales were included. Using molecular phylogenetic analyses based on chloroplast-encoded *rcbL* gene sequences, Daugbjerg *et al.* (1994) confirmed the separation of four of the six subgenera accepted presently (subgenera *Macrura* Hori, Moestrup & Hoffmann and *Hexactis* Hori, Moestrup & Hoffmann are both monotypic, containing *P. longicauda* van Meel and *P. virginica* Pennick, respectively, but they were not included in that study). It should be noted here that Sym & Pienaar

(1997) questioned the taxonomic validity of *Macrura*. Later, analyses of nuclear-encoded SSU rDNA sequences also supported the division of the genus into subgenera (e.g. Bhuiyan *et al.*, 2015). Thus, at least two genes from different genetic compartments support the synapomorphic status of the morphological characters used to distinguish subgenera.

In studies by Stonik & Aizdaicher (2005) and Orlova *et al.* (2009) six species of *Pyramimonas* were recorded in far-eastern Russia. Two of these, *P. aurita* Daugbjerg and *P. aff. cordata* McFadden, Hill & Wetherbee, were present at concentrations greater than 1×10^6 cells l^{-1} during certain months of the year (Orlova *et al.*, 2009). Here we describe a novel species of *Pyramimonas* (*P. tatianae*) from Golden Hope Bay in the vicinity of Vladivostok, using morphological features from light and transmission electron microscopy in combination with molecular phylogenetics based on chloroplast-encoded *rbcL* sequences. We show *P. tatianae* to be a new member of the subgenus *Vestigifera* related to but distinct from *P. mitra* and *P. cordata* McFadden. Most likely *P. aff. cordata sensu* Orlova *et al.* (2009) is conspecific with *P. tatianae*. We also provide a formal description of the class Pyramimonadophyceae, which comprises both extant and extinct genera.

Materials and methods

Organism

The scaly green quadriflagellate studied here was isolated from a water sample collected on 14 June 2000, in Golden Horn Bay near Vladivostok, far eastern Russia (Fig. 1). The water temperature was 15°C and the salinity 30. A clonal culture was established by Nina A. Aizdaicher and brought to the Dept of Biology, University of Copenhagen by Dr Tatiana Yu

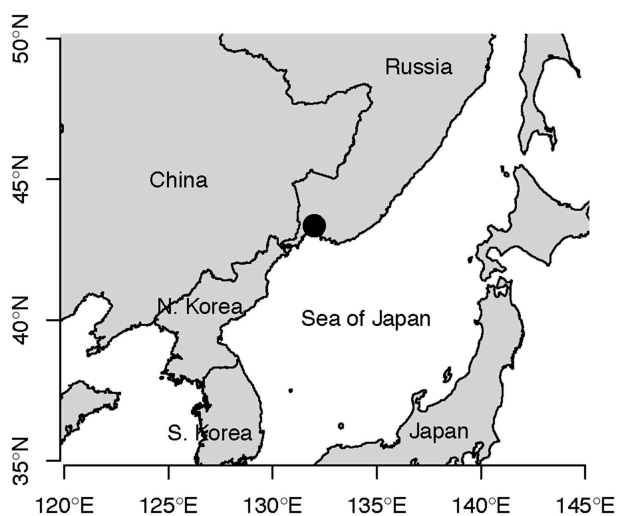


Fig. 1. Map showing position of the type locality of *Pyramimonas tatianae* sp. nov. from Golden Hope Bay (filled circle) near Vladivostok, far eastern Russia.

Orlova for further studies. It was maintained in L1 medium (Andersen *et al.*, 2005) for many years but recently the culture was unfortunately lost.

Light microscopy

Live cells were viewed under an Olympus BX51 microscope equipped with differential interference contrast and a $\times 60$ oil immersion objective (NA = 1.4). Photographs were taken with a digital camera from Zeiss (model HRc).

Electron microscopy

Body and flagellar scales were studied by preparing whole mounts with material fixed in osmium vapour (4%) and subsequently stained in aqueous uranyl acetate (2%). See Moestrup & Thomsen (1980) and Daugbjerg & Moestrup (1992a) for details. The ultrastructure of thin sectioned material followed the protocol used by Daugbjerg & Moestrup (1992a). Thin sections were stained first in uranyl acetate for 10 min at 70°C, followed by staining in lead citrate for the same period of time at the same temperature. The material was examined in a JEOL JEM-1010 electron microscope operated at 80 kV (Jeol, Tokyo, Japan), and images were taken with a Gatan BioScan Camera model 792.

DNA extraction and amplification

Total genomic DNA was extracted as previously outlined in Hansen *et al.* (2018). Approximately 1400 base pairs of the chloroplast-encoded *rbcL* gene were amplified using the forward primer Pra 1F (5'-ATGKCACCAMAAACWGARACKAAA-3') and the reverse primer Pra 1409R (5'-AAAYTCRAAYTTAATYTCTTTC-3'). These primers were designed for this study. The amplification was performed using the 5X Hot FIREPol Blend Master Mix from Solis BioDyne. Thermal conditions for the amplification included 1 initial cycle for denaturation at 95°C for 12 min. This was followed by 35 cycles each consisting of a denaturation step at 95°C for 10 s, an annealing step at 41°C for 30 s and an elongation step at 72°C for 60 s. A final elongation step included 5 min at 72°C. The expected length of the PCR-amplified product was confirmed by electrophoresis using an agarose gel with a final concentration of 1.5%. Amplified fragments were stained with GelRed and visualized in a gel documentation XR system from BioRad (Hercules, California, USA) alongside the 100 base pair RAIN-BOW eXtended DNA ladder in a separate slot.

Purification and sequence determination

Purification of the *rbcL* gene used ultrafiltration by applying the Nucleofast 96 PCR kit from Macherey-Nagel following the recommendations of the

manufacturer. The concentration of the PCR-amplified product was measured with a P300 NanoPhotometer (Implen GmbH, Munich, Germany). The chloroplast gene was determined in both directions using the amplification primers. The service provided by MacroGen Europe was used for sequence determination.

Phylogenetic inference

The *rbcL* sequence of *P. tatarica* was added to a data matrix comprising a diverse assemblage of *Pyramimonas* species for which the *rbcL* sequences are available in GenBank (Table 1). A total of 24 species were aligned with Clustal W (Larkin *et al.*, 2007) and further edited using Jalview (ver. 14, Waterhouse *et al.*, 2009). *Cymbomonas tetramitiformis* formed the outgroup taxon. The data matrix comprised 1089 base pairs and was analysed using Bayesian analysis (BA) and maximum likelihood (ML). For BA, MrBayes (ver. 3.2.6, Ronquist & Huelsenbeck, 2003) was set to run for a total of 10 million generations and a tree was sampled every 1000 generations. The burn-in value was decided by plotting LnL scores as a function of generations and it converged after 501 000 generations. This left 9500 trees for making a 50% majority-rule consensus tree. In jModelTest (ver. 2.1.3, Darriba *et al.*, 2012) the parameter settings for the best model for ML analysis were suggested to be GTR-I-G (I=0.432 and G=1.85). PhyML (Guindon *et al.*, 2010) was used for ML bootstrap analyses (1000 replications) and this phylogenetic inference was run on the Montpellier bioinformatics platform available at www.atgc-montpellier.fr/phyml. Bootstrap values were mapped onto the tree topology from Bayesian analysis.

Results

Pyramimonas tatarica Daugbjerg, Fassel & Moestrup sp. nov.

Description

Cells 6–7 μm long and 5–6 μm wide. Cell outline with truncated anterior part, nearly parallel sides and rounded posterior. Four flagella emerge from an apical flagellar pit 0.3 \times cell length. In non-swimming mode flagella bend backwards, their length 1.3 times the cell length. Chloroplast single, green in colour and anteriorly split into four lobes of approx. half the chloroplast in length. Posterior, centrally located pyrenoid, surrounded by starch, with thylakoids penetrating the matrix anteriorly. Eyespot single, red and positioned near pyrenoid in posterior end of the cell, not associated with a chloroplast lobe. Cell body covered by four scale types: small square underlayer scales in the flagellar pit,

rod-shaped footprint scales, box and crown scales. Box scales with non-perforated rims, the floor with lines forming a square surrounding an additional ~5 parallel lines attach comb-like to another line. Crown scales with two spines on each of four struts that unite distally with a spine projecting upwards and a free hanging rod projecting downwards. Flagella covered by three types of scales: underlayer of small pentagonal scales covered by limuloid scales. Each limuloid scale with central spine and two short lateral spines directed towards the anterior end of the flagellum. The base plate of the limuloid scale non-striated, with a small perforation near the central spine. Two opposite rows of bi-partite, unsegmented hair scales also covered the flagella. No cyst or palmelloid stages noted.

HOLOTYPE: A fixed sample of *P. tatarica* embedded in Spurr's resin has been deposited at the Botanical Museum, University of Copenhagen and serves as type material. It was given the reference number C-A-92103. **TYPE LOCALITY:** Golden Hope Bay, near Vladivostok, far eastern Russia.

ETYMOLOGY: Named after Tatiana Yu Orlova in recognition of her many contributions to our understanding of phytoplankton communities in far eastern Russia.

Live microscopy

Live cells were green, with an almost spherical outline except for the truncated apical end. Cells were 6–7 μm long and 5–6 μm wide ($n = 10$) (Figs 2–6). The chloroplast was cup-shaped with four lobes extending from the cell middle to near the apical end (Figs 2–3). A large pyrenoid completely covered by starch grains was positioned in the middle of the antapical end (Figs 2–6). In most cells the single eyespot was visible adjacent to the upper part of the pyrenoid, embedded in the chloroplast matrix (Figs 2–5). A large vacuole, most likely the scale reservoir, could be seen in the upper part of the cell (Fig. 5). The flagellar pit was 2–2.5 μm deep (Figs 2–4, 6). Four flagella emerged from the pit and in the relaxed (non-moving) state bent strongly at approx. half length (Figs 2–6). The angle of the flagellar bend varied between 90 and 170° and the flagella were approx. 1.3 \times cell length. The flagella were evenly spaced in four directions (Figs 7–8). In optical cross section, cells were square with rounded corners (Figs 7–9). Dividing cells near completion of cytokinesis were shown in Figs 10–11. A large aggregate of red-coloured droplets was sometimes observed during division (Fig. 11), perhaps representing a dividing eyespot.

Swimming behaviour

Cells viewed under the light microscope swam as is typical for many species of the subgenus *Vestigifera*. During forward swimming they rotated their

Table 1. List of *Pyramimonas* spp. included in the phylogenetic inference based on chloroplast-encoded *rbcl* sequences. Division into subgenera, geographic origin and GenBank accession numbers are also provided.

Subgenus	Species (each subgenus in alphabetical order)	Geographic origin	GenBank accession number
<i>Pyramimonas</i> McFadden	<i>P. cyrtoptera</i> Daugbjerg	Foxe Basin, Canada	L34819
	<i>P. octopus</i> Moestrup & Kristiansen	Wadden Sea, Denmark	L34817
	<i>P. propulsa</i> Moestrup & D.R.A. Hill	Port Phillip Bay, Australia	L34777
	<i>P. tettraryncus</i> Schmarida	Village pond, Ejby, Denmark	L34833
	<i>P. vacuolata</i> S. Suda, Horiguchi & Sym	Okinawa, Japan	LC015748
<i>Vestigifera</i> McFadden	<i>Pyramimonas</i> sp. (strain Te2Py)	Okinawa, Japan	LC015749
	<i>P. cycloreteta</i> Daugbjerg	Foxe Basin, Canada	L34814
	<i>P. diskoicola</i> Hardardottir, N. Lundholm, Moestrup & T. G. Nielsen	Disko Bay, Greenland	KP792648
	<i>P. mantoniae</i> Moestrup & D.R.A. Hill	Port Phillip Bay, Australia	L34810
	<i>P. mitra</i> Moestrup & D.R.A. Hill	Corner Inlet, Australia	L34812
<i>Trichocystis</i> McFadden	<i>P. moestrupii</i> McFadden	Norman Bay, Australia	L34811
	<i>P. orientalis</i> Butcher	?	L34813
	<i>P. tatiana</i> Daugbjerg, Fassel & Moestrup	Golden Horn Bay, eastern Russia	MK990598
	<i>P. tychotreta</i> Daugbjerg	Weddell Sea, Antarctica	L34778
	<i>Pyramimonas</i> sp. 'Greenland'	Disko Bay, Greenland	L34818
	<i>P. australis</i> Andreoli & Moro	Terra Nova Bay, Antarctica	AJ404887
	<i>P. cirolanae</i> N.C. Pennick	Port Phillip Bay, Australia	L34776
	<i>P. grossii</i> Parke	Corner Inlet, Australia	L34779
	<i>P. parkeae</i> R.E. Norris & B.R. Pearson	Hachijo Island, Japan	KX013546
	<i>P. olivacea</i> N. Carter	?	L34815
<i>Punctatae</i> Sym & Pienaar	<i>P. aurea</i> S. Suda	Palau islands, Republic of Palau	AB052290
Undescribed subgenus I <i>sensu</i> Suda <i>et al.</i> , 2013	<i>P. mucifera</i> Sym & Pienaar (strain TUP12)	Urata, Japan	LC032456
Undescribed subgenus II <i>sensu</i> Suda <i>et al.</i> , 2013	<i>P. formosa</i> Sym & Pienaar	Australia	L34834
Outgroup	<i>Cymbomonas tetramitiformis</i>	?	KX013545

longitudinal axis and when they stopped briefly, swimming was resumed in a different direction.

Body scales

The cell membrane of the flagellar pit was covered by an innermost layer of square body scales, ~40 nm in width (Figs 14 (arrowhead), 39). Outside the flagellar pit these small square body scales were lacking (compare Fig. 39 with Fig. 37). The cell body was completely covered by tightly packed layers of box-shaped scales (Figs 15–17, 21). The floor of the box scales measured ~250 nm in length and width, whereas the length and width across the distal part of the rim measured ~295 nm (Figs 13–14). Hence, the rims formed an angle of 120–125° relative to the floor (Fig. 16). The rims were non-perforated (Fig. 17) and 75 nm high. The proximal side of the scale floor was without markings (Fig. 14). The distal side showed an arrangement of lines that included an outer square and inside this a line to which five perpendicular lines were connected (Figs 13, 15 and 42). Rod-shaped 'footprint' scales were positioned between the box scales and measured ~100 nm in length and 22 nm at their widest part (Fig. 15 (arrowheads), Fig. 18). The outermost layer was composed of crown scales, measuring ~275 nm in length and width and ~210 nm in height including the distal central spine (Figs 21, 23). The four struts forming the proximal part comprised a square with rounded corners (Fig. 23). Two downward pointing spines were present on each of the four struts (Figs 19, 23). From the middle

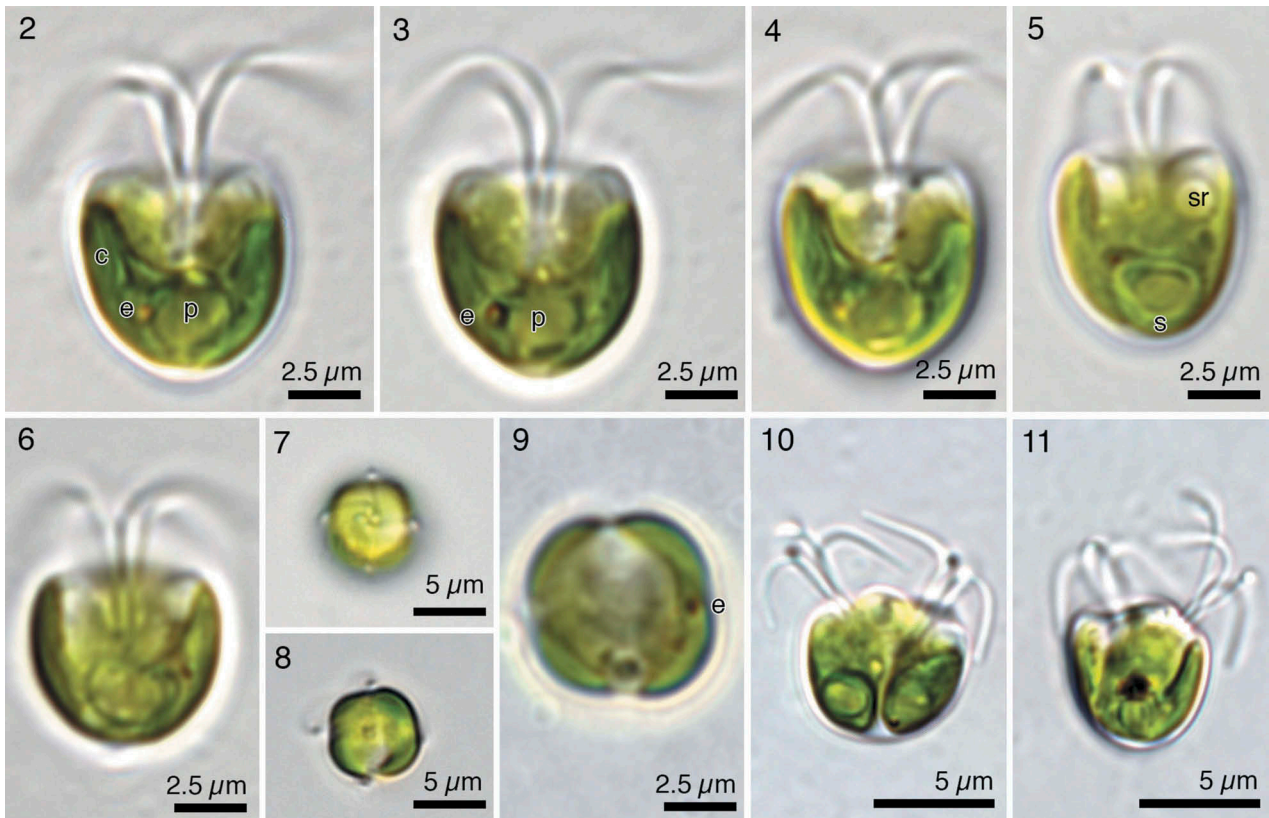
of each of the four sides an upright arm, each with two upward pointing spines, adjoined at the scale midpoint. Here a central free-hanging central strut was present, and there was a large spine above the point where the upright arms adjoined.

Flagellar scales

The flagella were covered completely by two scale layers, an inner layer of small pentagonal under-layer scales (Fig. 24) and an outer layer of limuloid scales (Figs 24–25). Each limuloid scale had a main slightly raised spine, with a short spine on either side of the main spine (Fig. 24). The limuloid scale floor lacked striations. However, a single perforation was noted in the scale floor near the base of the main spine (Figs 24–25). On the flagella the limuloid spines partly overlapped by a quarter (Fig. 25). They were 325 nm long and 215 nm wide at the widest part. Flagellar hairs were 920 nm long and 12 nm wide (Figs 26, 27). They were composed of three parts, a proximal triangular part (~55 nm long) and a ~550 nm long almost evenly thick middle part and a somewhat shorter (~320 nm long), thinner distal part (Fig. 26).

Cell ultrastructure

The truncated apical end, the almost parallel sides and the rounded antapical end were also evident in cells fixed in osmium vapour and viewed in the electron microscope (Fig. 12). The general ultrastructure and



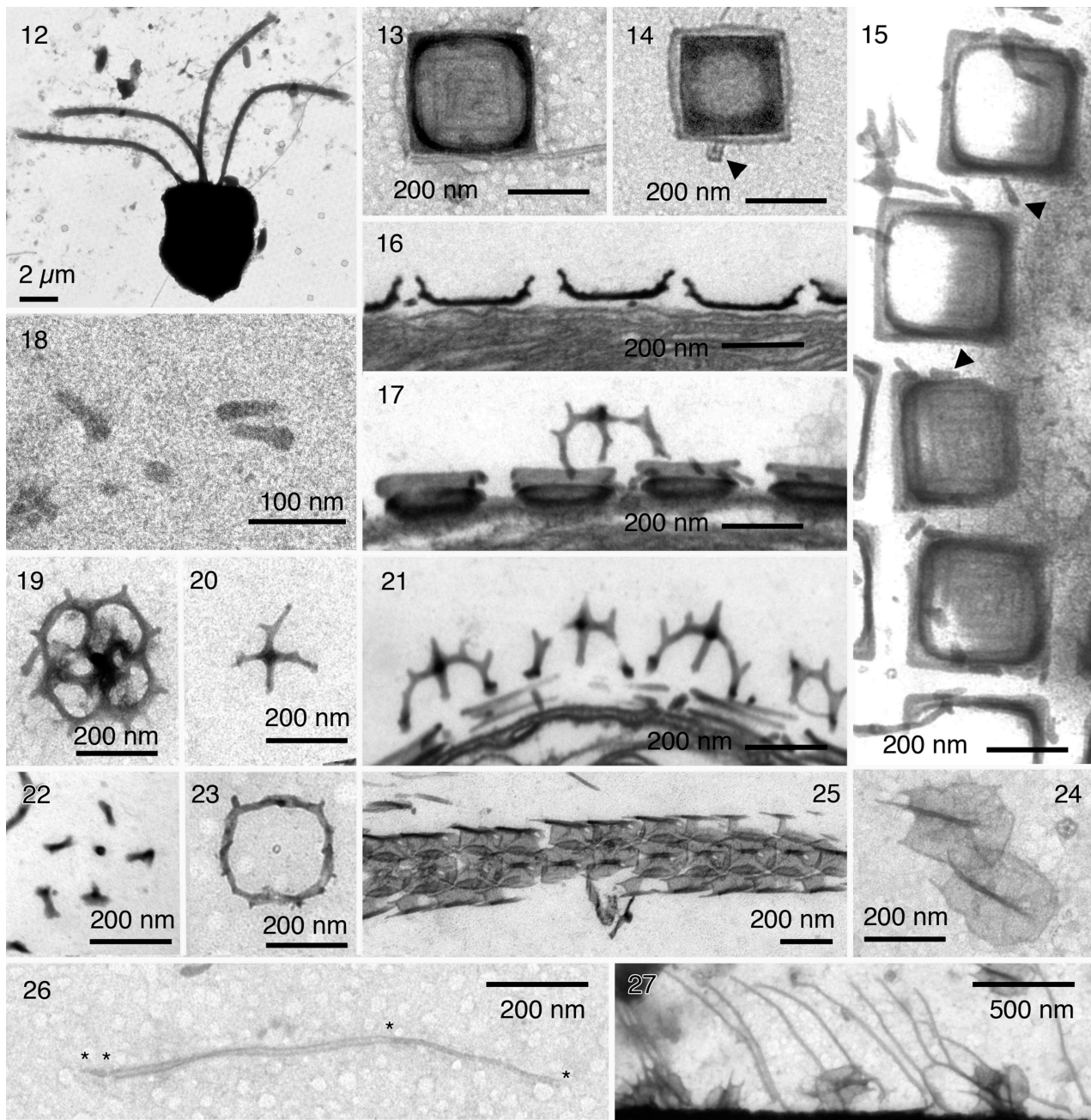
Figs 2–11. Light micrographs of *Pyramimonas tatiana* sp. nov., live cells in Nomarski interference contrast. **Figs 2–6.** Optical longitudinal sections showing cell outline, position of flagella in resting cells, extension of the single cup-shaped chloroplast (c), pyrenoid (p) surrounded by starch sheet in antapical end, and scale reservoir (sr) in apical end. The single eyespot (e) is located near the pyrenoid (middle in Figs 2–3 and above in Figs 4–5). **Figs 7–9.** Optical transverse sections. **Figs 7–8.** Two images through the flagellar pit area showing the arrangement of flagella in a resting cell. **Fig. 9.** Section through the region with the eyespot (e). Note the two chloroplast lobes on the left side of the cell. On the right side the lobes have fused. **Figs 10–11.** Optical longitudinal sections through division stage. The flagella have been replicated and cytokinesis is approaching. Note two pyrenoids in Fig. 10 and a large aggregate of red-coloured droplets in Fig. 11.

thus the disposition of cell organelles was revealed from a series of transverse (Figs 28–33) and longitudinal sections (Figs 34–39). The division of the single chloroplast into four lobes was clearly visible in cross sections through the anterior part of the cell (Figs 28–29). Thin sections confirmed that at a level below the flagellar pit the individual chloroplast lobes had fused (Fig. 30) to form a cup-shaped chloroplast (Figs 34–35). The chloroplast closely adjoined the antapical end of the cell (Figs 34–37) and posterior vacuoles were not observed. In the flagellar pit four almost evenly spaced flagella could be discerned (Fig. 28). Two dictyosomes were located on opposite sides of the flagellar pit (Fig. 28), almost the length of the flagellar pit (Fig. 37). A large elongated, parietal nucleus was visible in many sections (Figs 28–29, 34, 36–37) and in one image was seen to occupy a little over 2/3 of the cell length (Fig. 36). The pyrenoid matrix was penetrated by thylakoids anteriorly (Fig. 36) in an arrangement that matches Type 1 *sensu* Hori *et al.* (1995). The eyespot consisted of droplets and was positioned at the same level as the pyrenoid (Fig. 33). A starch sheet surrounded most of the pyrenoid matrix, leaving only the anterior part free (Figs 34–36). A dividing cell with two pyrenoids each surrounded by starch

was illustrated in Fig. 37. Lipid droplets were occasionally seen (Fig. 28). Profiles of mitochondria could be seen throughout the cell matrix (Figs 28–30, 34–37) and they probably formed a reticular network. A scale reservoir was present at the level of the flagellar pit (Figs 31, 35–36) and profiles of flagellar scales could be seen being released to the cell exterior via the flagellar scale reservoir duct (Fig. 38). The flagellar basal bodies were arranged in a rhomboid, the two central basal bodies joined by a rectangular synistosome (Fig. 32). The basal bodies were arranged in parallel and emerged from the base of the flagellar pit (Fig. 39). They were ~830 nm long. The flagellar apparatus was not studied in detail.

Drawings of cell and body scales

For reasons of comparison with other species of *Pyramimonas* the general cell outline, disposition of major organelles and five of seven body scales were illustrated in Figs 40–45. The reconstructions were based on whole mounts of complete scales (Figs 13–14, 18–19, 24 and 26–27) and sectioned material (Figs 15–17, 20–23 and 25).

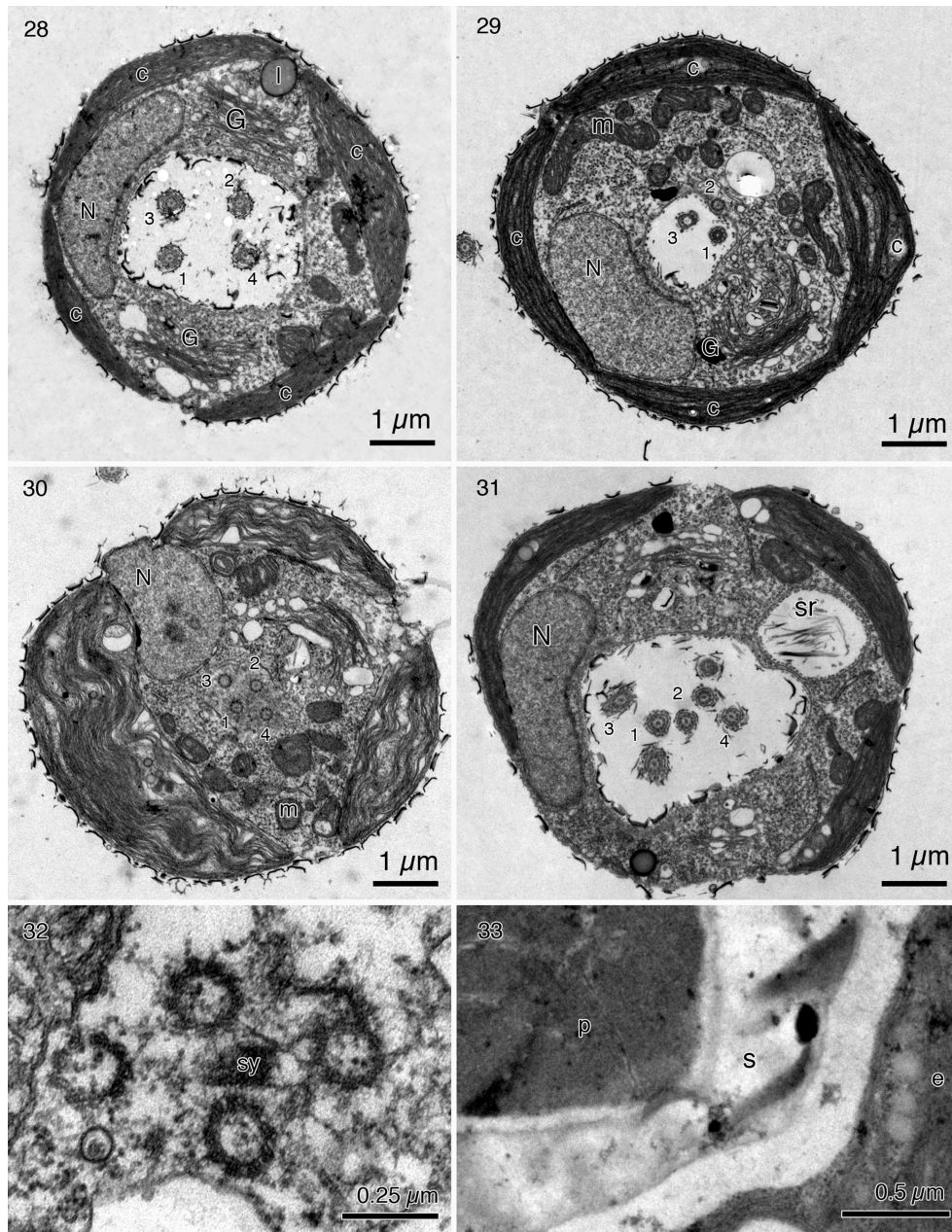


Figs 12–27. Transmission electron microscopy of whole cell, body and flagellar scales in *Pyramimonas tatianae* sp. nov. Figs 12–14, 18–19, 24 and 26–27. Uranyl acetate-stained whole mounts. Figs 15–17, 20–23, 25. Thin-sectioned material. **Fig. 12.** Whole cell. **Figs 13–17.** Box scales, note slight variation in the box scale floor, and solid rims. A small square body scale is indicated by an arrowhead in Fig. 14 and two footprint scales are marked by arrowheads in Fig. 15. **Fig. 18.** Footprint scales. **Figs 19–23.** Crown scales. Note central, hanging, hollow strut and lack of basal cross in the proximal square base which has rounded corners. **Figs 24–25.** Limuloid scales, each possessing a small perforation and no ornamentations except for the two small apical spines on each side of the slightly raised main spine. A flagellar underlayer scale is marked by an arrowhead in Fig. 24. **Figs 26–27.** Flagellar hair scales. The three parts are indicated by asterisks. Note triangular proximal part on the left.

Molecular phylogeny

Owing to poor support from posterior probabilities and bootstrap values, the relationship between the four described and the two undescribed subgenera of *Suda* *et al.* (2013) was unresolved. This prevented a discussion of the direction of the evolutionary history of the subgenera, and identification of ancestral and derived states. In contrast, the six subgenera included in this

study each received high to relatively high support (Fig. 46) for monophyly, although they were originally based on morphological features only. Specifically, the species of interest in this study, *P. tatianae* formed a sister taxon to *P. mitra*. This relationship was highly supported by posterior probability (PP = 1.0) but less so by bootstrap (BS = 72%). *P. tatianae* clustered together with other species belonging to the subgenus *Vestigifera*.

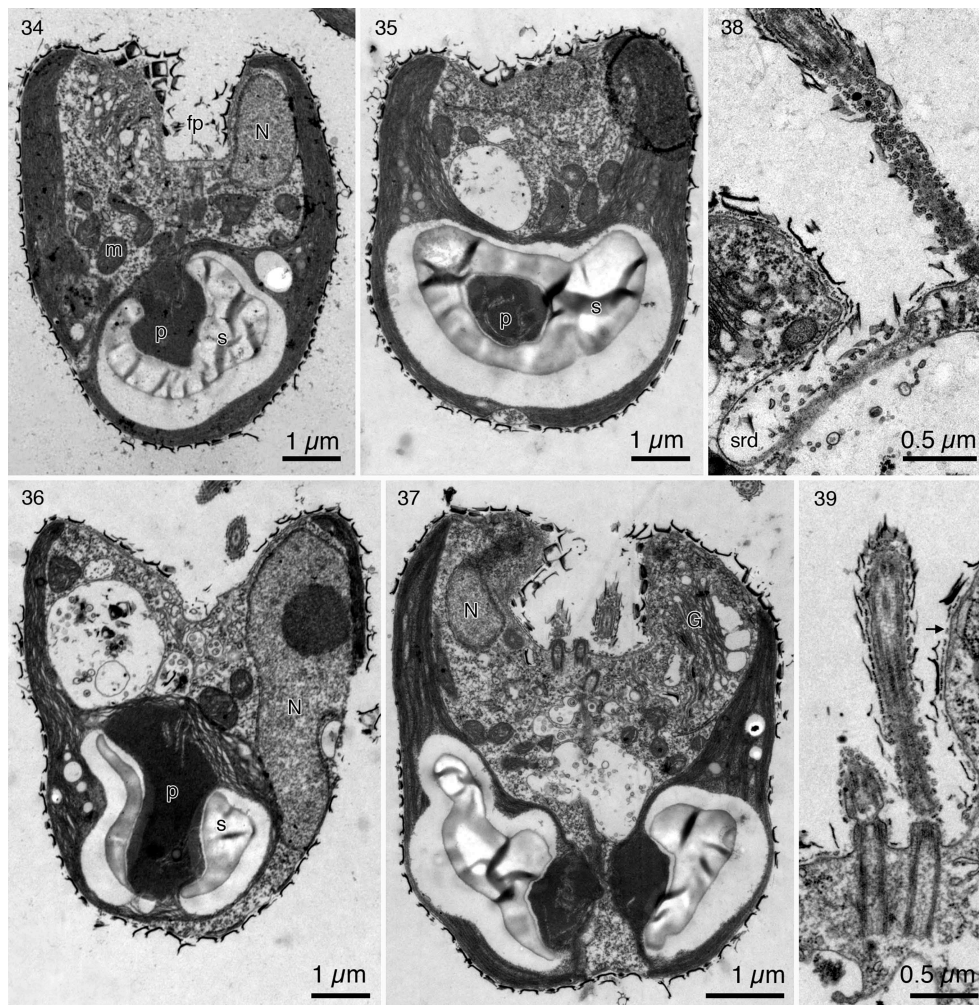


Figs 28–33. Cross sections and details of the arrangement of basal bodies and eyespot in *Pyramimonas tatianae* sp. nov. (transmission electron microscopy). **Figs 28–30.** Sections through different levels of the flagellar pit and basal bodies. Nucleus is located in the cell perimeter. Also visible are the four chloroplast lobes (c) (only three in Fig. 30), two Golgi bodies (G), mitochondrial profiles (m) and a single lipid droplet (l). The flagellar basal bodies have been numbered. Cells shown in Figs 29–30 are completely covered by a layer of box scales. **Fig. 31.** Dividing cell showing 7 of 8 flagella. Note scale reservoir (sr) containing flagellar hair scales. **Fig. 32.** Section through basal bodies at the level of the synistosome (sy). A few interconnecting fibres are also visible. **Fig. 33.** Section at the level of the eyespot (e) comprising a number of carotenoid droplets. Parts of the pyrenoid (p) and the starch sheet (s) are also visible.

Within this subgenus two subclades were recovered, both with high support values. One lineage comprised four cold-water species and *P. orientalis* (supported by PP = 1.0 and BS = 91%) while the other lineage comprised temperate to subtropical species (supported by PP = 1.0 and BS = 99%). The cold-water species comprised both arctic and antarctic species. The arctic species did not form a single lineage, as *P. diskoicola* from Disko Bay was more closely related to *P. tychotreta* from Antarctica than to other arctic species, even some isolated from the same area.

Sequence divergence

We estimated the sequence divergence to further elucidate the genetic differences between *P. tatianae* and the most closely related species. In pair-wise comparisons *P. tatianae* differed by 3.0% from *P. mitra*, 2.5% from *P. mantoniae* and 5.7% from *P. moestrupii* (calculations based on Kimura-2-parameter model). Using MEGA (ver. X, Kumar *et al.*, 2018) we calculated the within group mean distances for subg. *Vestigifera* (7.7%), subg. *Trichocystis* (9.9%) and subg. *Pyramimonas* (12.5%).



Figs 34–39. Longitudinal sections through *Pyramimonas tatianae* sp. nov. (transmission electron microscopy). **Figs 34–36.** Three different cells revealing the position of nucleus (N) and antapical extension in Fig. 36, flagellar pit (fp), posterior pyrenoid matrix penetrated by thylakoids (p) and surrounded by a starch sheet (s), mitochondria (m). **Fig. 37.** Section through dividing cell with separated chloroplasts each containing a pyrenoid partly surrounded by starch. A large Golgi body (G) is visible in the apical end. **Fig. 38.** Scale reservoir duct containing underlayer scales and sectioned parts of limuloid scales. **Fig. 39.** Section through two flagella and their basal bodies revealing a layer of pentagonal underlayer flagellar scales and an outer layer of limuloid scales. The underlayer body scales can be discerned in the top, right and one has been indicated by an arrow.

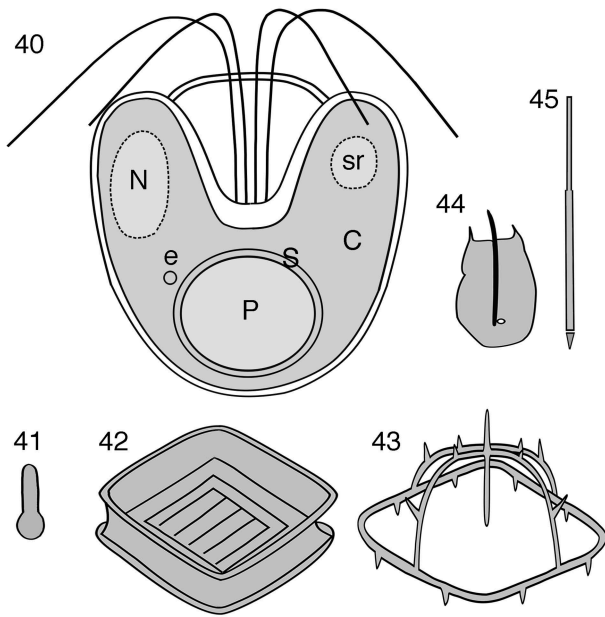
The differences were to some extent reflected in the average branch lengths within the subgenera.

Discussion

Comparison with related, similar species

The general cell morphology and in particular the body scales and phylogenetic position based on chloroplast-encoded *rbcL* favoured a novel identity of *P. tatianae*. However, *P. tatianae* shared a number of features with other vestigiferans. In a study of the phytoplankton community of Amurskii Bay, Orlova *et al.* (2009) recorded a species, which they identified as *P. aff. cordata*. In their table 2 (p. 75), they noted that it could represent a new species due to the unique floor of the box scale (no illustrations

available) and a different sterol composition compared to *P. cordata* McFadden, which had been characterized by Ponomarenko *et al.* (2004) some years before. *P. tatianae* and *P. cordata* are similar in cell dimensions (7 μm in length and 5 μm in width) and they possess a single eyespot. However, the general outline of the cells was different. In *P. tatianae* the sides were almost parallel and the antapical part rounded, whereas in *P. cordata* the sides formed an angle and the antapical end was therefore more pointed. The eyespot was positioned in the anterior part and adjacent to the nucleus in *P. cordata*, whereas in *P. tatianae* the eyespot was located in the posterior part and adjacent to the pyrenoid. The morphology of the box and limulus scales was also different (compare Figs 13–15 and 24 with figs 2C, F and H in McFadden *et al.*, 1986). Based on this



Figs 40–45. Schematic drawings of *Pyramimonas tatianae* sp. nov. **Fig. 40.** The cell showing the disposition of major organelles (N = nucleus, C = chloroplast, P = pyrenoid, S = starch, e = eyespot, sr = scale reservoir). **Fig. 41.** Rod-shaped footprint scale. **Fig. 42.** Box scale. **Fig. 43.** Crown scale. **Fig. 44.** Limuloid scale. **Fig. 45.** Flagellar hair scale.

comparison and on Orlova *et al.* (2009), it is very plausible that *P. aff. cordata* and *P. tatianae* are conspecific. This is further supported by the fact that they were sampled in Amurskii Bay. Additionally, *P. tatianae* was isolated in June, where previously it has been known to occur in high cell abundances (5×10^5 – 1×10^6 cells l^{-1}) as *P. aff. cordata*.

A few other species of *Vestigifera* also possess crown scales with a central strut that extends downwards without attaching directly to the proximal part (i.e. *P. mitra*, *P. cordata*, *P. nephroidea* and *P. diskoicola*). A detailed comparison revealed that the crown scale of *P. tatianae* most closely resembled that observed in *P. mitra*. The upright arms are flatter in *P. tatianae*, and there are four evenly distributed small spines pointing upwards on the proximal rim in *P. mitra*. The box scales in *P. mitra* to some extent resemble those in *P. tatianae* (low rims and non-perforated sides). In *P. mitra*, however, the box scale floor possesses two squares (outer and inner), each with a number of thin lines. In *P. tatianae* the scale floor possessed a square composed of a single line, and on the inside were approx. 5 lines adjoined perpendicularly to another line arranged at a right angle. Another marked difference relates to the position and number of eyespots. In *P. tatianae* the eyespot is single and positioned in the lower half of the cell, whereas in *P. mitra* it is double and positioned in the upper half of the cell. In cell dimensions *P. tatianae* and *P. mitra* overlap in width ($\sim 6 \mu m$) but *P. mitra* is slightly longer (6 – $10 \mu m$, versus 6 – $7 \mu m$ in *P. tatianae*). Therefore, morphology and sequence divergence estimates both support *P. tatianae* as a novel species. Table 2 has been compiled to highlight important morphological features that clearly separate *P. tatianae* from a number of similar species.

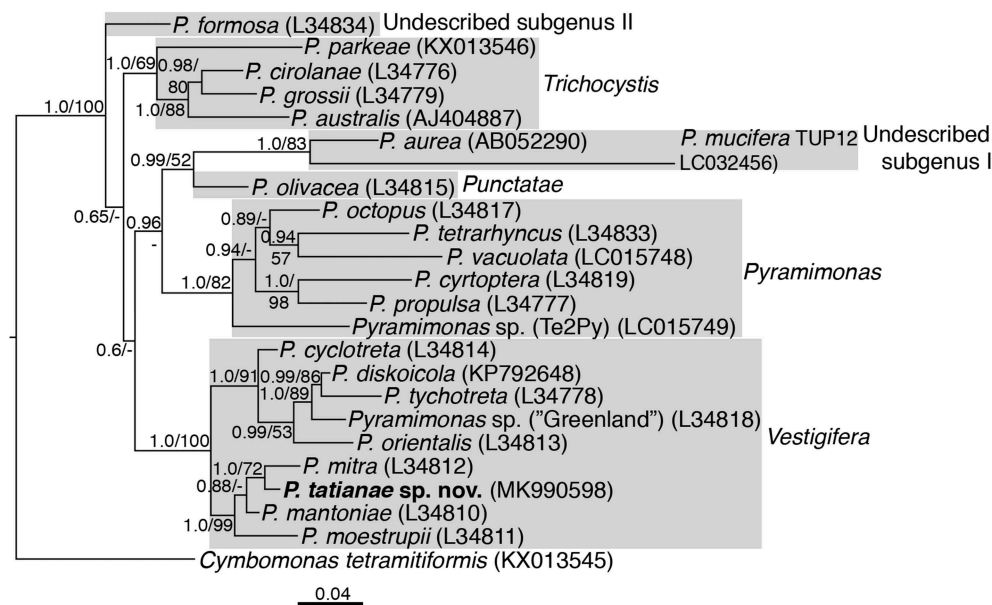


Fig. 46. Phylogeny of *Pyramimonas tatianae* sp. nov. (marked in bold) based on chloroplast-encoded *rbcL* sequences (1089 base pairs) and inferred from Bayesian analysis. The ingroup, which comprised 23 species of *Pyramimonas* belonging to four well-characterized and two undescribed subgenera, is indicated by the grey boxes. *Cymbomonas tetramitiformis*, another species belonging to Pyramimonadales, was used as outgroup. Posterior probabilities (PP ≥ 0.5) from Bayesian analysis and bootstrap values (BS $\geq 50\%$) from maximum likelihood analyses with 1000 replications are shown to the left of internal nodes. PP < 0.5 and BS values $< 50\%$ are indicated by a hyphen ('-'). GenBank accession numbers are written in parentheses. The branch lengths are proportional to the number of character changes.

Table 2. Morphological features of *Pyramimonas tatianae* compared to four similar species of the subgenus *Vestigifera*.

Species of <i>Pyramimonas</i>	Length (µm)	Width (µm)	Cell outline of antapical end	Number and position of eyespots	Limuloid scale: the floor	Box scale: the floor	Crown scale: total number of spines on upright arms	Crown scale: number of upward pointing spines on proximal rim
<i>P. tatianae</i> ¹	6–7	5–6	Rounded	1, posterior	Non-striated	Square surrounding ca. 5 parallel lines attach comb-like to another line	8	0
<i>P. mitra</i> ²	7–10	5.5–7	Rounded or pointed	2, anterior	Non-striated	2 concentric squares	8	4
<i>P. cordata</i> ³	7	5	Pointed	1, anterior	Striated	Raised square with cross and small perforations	12	0
<i>P. moestrupii</i> ³	7	5	Pointed	2, anterior	Non-striated	Central obelisk, radiating perforations	8	0
<i>P. mantoniae</i> ⁴	6–6.5	5–5.5	Pointed	2, anterior	Non-striated	4 elevations, larger central knob, lines running parallel to the sides of the box scale	No crown scales	No crown scales

¹This study; ²Moestrup & Hill (1991); ³McFadden *et al.* (1986); ⁴Moestrup & Hill (1993).

Species diversity of *Pyramimonas* in Russian far eastern waters

As mentioned above, a few studies have addressed the species diversity of *Pyramimonas* in far eastern Russia (e.g. Stonik and Aizdaicher, 2005; Orlova *et al.*, 2009). Six species were identified in a survey covering samples collected 1991–2006 in Amurskii Bay. One of these was *P. aurita* Daugbjerg, previously only known from North Foxe Basin, high Arctic Canada. *P. aurita* was the only species with high cell abundance recorded in Amurskii Bay ($1 \times 10^4 - 1 \times 10^6$ cells l⁻¹ in January to March). At the time of the bloom, the seawater temperature in the vicinity of Vladivostok (averaged over several years) never goes below -1.5°C or above 2.7°C (<https://www.seatemperature.org/asia/russia/vladivostok-march.htm>). This fits well with the temperature conditions in Northern Foxe Basin. As the temperature increases later in the year other species of *Pyramimonas* (viz. *P. tatianae*, as *P. aff. cordata* in Orlova *et al.* 2009), *P. amyliifera* Conrad, *P. grossii*, *P. semiglobosa* Pascher and *P. longicauda* Van Meel take over. The highest cell abundances were recorded in June–September when the seawater temperature range was $13.2\text{--}19.7^\circ\text{C}$. The species diversity of *Pyramimonas* described from far eastern Russia (six species) is similar to a diversity study of *Pyramimonas* species from Ryukyu Archipelago (southern Japan) by Suda *et al.* (2013), who described five species from Okinawa-jima Island.

Taxonomic history of subgenus *Vestigifera*

Since this subgenus was erected by McFadden *et al.* (1986) 10 new species have been added to the list, which therefore currently comprises 19 taxonomically accepted species (Guiry & Guiry, 2019). Hence,

Vestigifera is by far the most species-rich subgenus and the species have a wide biogeographic distribution which includes polar, temperate and subtropical waters. Morphological characters originally suggested to circumscribe the subgenus included: (1) an excentric pyrenoid invaded by a few thylakoids anteriorly; (2) a cup-shaped starch grain with two anterior lobes; (3) four basal bodies arranged in a diamond configuration and interconnected by a square synistosome; (4) type 1 underlayer scales in the flagellar pit; (5) footprint scales between box scales outside the flagellar pit; and (6) usually two, bi-layered, eyespots. These features have been shown to characterize all vestigiferan species studied since 1986 and thus represent stable morphological features (synapomorphies). Phylogenetically, it was shown by Daugbjerg *et al.* (1994) using chloroplast-encoded *rbcL* sequences and confirmed later by nuclear-encoded SSU rDNA sequences (e.g. Moro *et al.*, 2002), that *Vestigifera* forms a single lineage within the genus *Pyramimonas*. Morphology and genetic markers from two different genomic compartments therefore point to a common evolutionary history for vestigiferans. However, the relationship between the subgenera within *Pyramimonas* has not been resolved and additional genetic markers are needed here. McFadden *et al.* (1986) in their study of *Pyramimonas* also included analyses of accessory pigments (xanthophylls). Lutein was found to be present in most of the species examined, but this pigment was replaced by siphonein in *P. amyliifera*. The presence and distribution of xanthophylls in *Pyramimonas* was therefore not an indicator of phylogeny and the presence of lutein must be regarded as a plesiomorphic character. This may explain why more recent taxonomic studies on *Pyramimonas* have not included chemical analyses of xanthophyll composition.

Phylogeny of *Vestigifera*, dispersal routes of cold-water species

The tree topology from the phylogenetic inference based on *rbcL* showed that the monophyletic subgenus *Vestigifera* was divided into two well-supported lineages (Fig. 46), one comprising cold-water (cryophilic) species and the cosmopolitan *P. orientalis*, the other lineage species from temperate to subtropical waters. *P. tycho-treta*, a species presently known only from Antarctica (Weddell Sea (Daugbjerg, 2000) and Ross Sea (Daugbjerg *et al.*, 2000)) formed a sister-taxon to *P. diskoicola*, which is only known from Disko Bay in West Greenland (Harðardóttir *et al.*, 2014). The two species formed a sister group to an undescribed *Pyramimonas* species (*Pyramimonas* sp. 'Greenland') from West Greenland, and *P. cyclotreta* from Northern Foxe Basin, Arctic Canada (Daugbjerg & Moestrup, 1992b) branched off as the earliest species among these cryophilic vestigiferan species. Hence, based on the currently available molecular data it seems likely that the ancestor of the antarctic *P. tycho-treta* shared an evolutionary history with species of arctic origin. If so, the ancestor(s) of *P. tycho-treta* must have experienced a long southbound dispersal route from the Arctic to Antarctica. With information from the growth response to variation in temperatures (i.e. growth ceased between 8 and 12°C; Daugbjerg, 2000), this north to south dispersal seems unlikely to have occurred in surface waters. Also, some of the major surface currents in the Atlantic Ocean (Gulf Stream, Atlantic Current) run in the opposite direction if we consider the most direct dispersal. Transportation in the deep dark layers of the Atlantic Ocean is more likely, especially if it included species with an encystment stage as part of the life cycle.

Since this was first discussed by Daugbjerg *et al.* (1994) we have learned that the life cycle of *P. tycho-treta* includes a thick-walled spherical cyst stage. If the ancestors of *P. tycho-treta* also produced encystment stages, the long transportation from the Arctic to Antarctica suddenly seems plausible. The long spines present on the cyst scales (Daugbjerg *et al.*, 2000) may result in aggregation and thus faster sinking rates. Interestingly, the two other known species of *Pyramimonas* from Antarctica, *P. gelidicola* McFadden, Moestrup & Wetherbee (van den Hoff *et al.*, 1989; van den Hoff & Ferris, 2009) and *P. australis* (Moro *et al.*, 2002) also include spherical encystment stages in their life cycle. As in *P. tycho-treta*, the cysts are covered by unique types of square cyst scales. These possess four elongations, which extend from each of the four corners. Some of these even have hooks at the distal part (van den Hoff *et al.*, 1989). In *P. australis* the cyst scales are different and possess long slender spines (Moro *et al.*, 2002).

Nuclear-encoded SSU rDNA sequences of four strains of *P. gelidicola* are available in GenBank but unfortunately these can only be compared to two other vestigiferans (viz. *P. disomata* Butcher *ex* McFadden, Hill & Wetherbee and *P. diskoicola*). In the single phylogenetic study that included both cryophiles (Harðardóttir *et al.*, 2014), the relationship between them and their relationship to other prasinophyte and chlorophyte species was unresolved, inhibiting further discussions of the number of introduction events to antarctic waters based on this genetic marker. It will be interesting to determine the *rbcL* sequence of *P. gelidicola* to elucidate whether it clusters with *P. tycho-treta*, as this would favour a single introduction of vestigiferans to antarctic waters. *P. australis* belongs to subgenus *Trichocystis* and is therefore not directly related to any of the cryophilic vestigiferans and it may therefore have had a separate introduction to antarctic waters. Within subgenus *Trichocystis*, *P. parkeae* had an early divergence (Fig. 46) and it also produces encystment stages as part of its life cycle (Aken & Pienaar, 1981). Therefore, a cyst stage may also have been present in the ancestor of *P. australis*, establishing a platform for transportation under less optimal water temperatures. Based on the currently available data, at least two independent events have resulted in a north to south introduction of *Pyramimonas* to Antarctica. Future studies will have to uncover if additional dispersal routes have been involved in the evolutionary history of *Pyramimonas* and if cyst stages are always a characteristic feature of Antarctic species belonging to this genus.

Given that *P. orientalis* is widely distributed (Moestrup & Thomsen, 1974) and that it previously has been observed in Disko Bay, West Greenland by Thomsen (1982) and Harðardóttir *et al.* (2014) it is not surprising that it clusters together with the cold-water species.

Addendum: formal description and discussion of *Pyramimonadophyceae* classis nova

Pyramimonas is one of the most species-rich genera of scale-bearing green algae. It was included by Christensen in the paraphyletic class Prasinophyceae, a group considered to having given rise to the different groups of more advanced green algae (Christensen, 1980–1994). The class was formally described by Thronsen & Moestrup (1988) but had already been raised to division level by Round (1971). As paraphyletic groups have gradually been disappearing from molecular phylogenetic trees, the clades comprising the different genera of prasinophytes have been given formal names, often at the class level. The phylogenetic tree of Marin & Melkonian (2010) shows the

prasinophytes to be distributed into eight clades. One of these, sometimes known as the monotypic class Mesostigmatophyceae (Marin & Melkonian, 1999), forms the base of the evolutionary line the Charophyta, which is thought to lead towards the land plants. The other prasinophyte clades all belong in the Chlorophyta and they presently comprise six classes, in addition to two groups referred to lower taxonomic levels. The six classes are Nephroselmidophyceae (Cavalier-Smith 1993) [Nephrophyceae], Chlorodendrophyceae (Massjuk 2006), Mamiellophyceae (Marin & Melkonian 2010), Palmophyllophyceae (Leliaert *et al.*, 2016), Picocystophyceae (Dos Santos *et al.*, 2017) and Chloropicophyceae (dos Santos *et al.*, 2017).

The remaining, class-less, groups are the order Pseudoscourfieldiales, termed clade V by Marin & Melkonian (2010), and the order Pyramimonadales (clade I).

Molecular studies have consistently shown these groups to be monophyletic, but the position of the two groups within the Chlorophyta is somewhat variable. The Pseudoscourfieldiales comprises two genera, *Pseudoscourfieldia* and *Pycnococcus*, which share the very unusual ultrastructural feature of invagination(s) of a mitochondrion into the pyrenoid matrix. While this is a rare arrangement in algae, the same feature was illustrated by Hasegawa *et al.* (1996) in *Prasinoderma* of the Palmophyllophyceae, a class which according to the molecular trees is not closely related to Pseudoscourfieldiales. Another feature that appears to be shared by the two genera is the two anisokont, posterior flagella. Whether these features suffice to elevate the Pseudoscourfieldiales to a higher level remains uncertain.

The second order, the Pyramimonadales, is a well-defined monophyletic group in molecular trees, and its members share a number of morphological features, which justifies raising of the order to the class level enjoyed by most other prasinophytes. It cannot be included in any of the recently (1993–2017) described classes. As mentioned below, this group contains a large number of fossil species. In recent phylogenetic molecular trees, based on a large number of genes (Nakayama *et al.* 2007; Leliaert *et al.*, 2016; Dos Santos *et al.*, 2017), the Pyramimonadales formed a well-supported sister group to the Mamiellophyceae. The relationship in some trees received high bootstrap support. An apparently shared feature of the two classes is the presence of spiny, superficially somewhat similar, flagellar scales in both the Pyramimonadales and in *Mamiella* of the Mamiellophyceae. However, details are different. The ‘limuloid’ scales of *Mamiella* are spider-web scales with a single spine, unlike the more complex scales of the Pyramimonadales, and the similarity may not indicate phylogenetic relationship.

The Pyramimonadales presently comprises the flagellate genera *Pyramimonas*, ‘*Prasinopapilla*’, and *Cymbomonas*, in addition to the coccoid genera *Pterosperma*, *Halosphaera* and *Pachysphaera* (the *Pterosperma* group). Species of the latter group reproduce by formation of flagellate cells (‘zoospores’), and flagellate cells of the six genera share many morphological traits. The coccoid stage of the *Pterosperma* group, known as the phycoma stage, is not a resting stage but a photosynthetic, initially single-celled stage which in some species may attain very large size, thus in *Halosphaera viridis* reaching 800 µm in diameter when mature (Parke & Hartog-Adams, 1965). The phycoma stage is one of the most unusual cells known in the green algae, but it remains uncertain whether it is part of a sexual stage, although this appears likely. While all flagellate cells in the Pyramimonadales have four flagella (or a multiple of four), very small uni cells have been reported in a culture of *Cymbomonas* and may represent gametes (Moestrup *et al.*, 2003). Fusion of the ‘gametes’ was not observed but resting cysts were formed in the culture, although the ability to form unicells and cysts was soon lost in the culture. An elongate uniflagellate stage tentatively suggested to represent a gamete has also been observed in wild material of *P. tychoetra* (Daugbjerg *et al.*, 2000). Fossil spores resembling the phycoma stage constitute some of the oldest known green algae, which extend back into the Precambrian (Tappan, 1980). Thus Permian ‘white coal’ or tasmanite (from Tasmania) contains spore-like cells which have been referred to the *Pterosperma* group (Tappan, 1980). The Pyramimonadales may therefore constitute one of the oldest groups of prasinophytes. A feature shared by all extant members of the Pyramimonadales is the presence of limuloid flagellar scales, the name given because of their resemblance to the marine invertebrate *Limulus*. Limuloid scales are arranged in 11 longitudinal rows on the flagella (see reconstruction of the flagellar surface by Moestrup & Hill (1993)), each scale bearing one larger and 1–2 smaller spines directed towards the flagellar tip. In the molecular tree of Marin & Melkonian (2010), species of the Pyramimonadales grouped together with a bootstrap value of 98–99%. Based on present evidence, morphological and molecular, it appears justified to raise the Pyramimonadales to class level, as the Pyramimonadophyceae *classis nova*. When the many fossil species and genera are included, it becomes one of the largest classes of prasinophytes. Fossil members of the other prasinophyte classes are unknown.

Pyramimonadophyceae Moestrup & Daugbjerg *classis nova*

Flagellates or coccoids, the latter reproducing by motile cells. Flagella covered with submicroscopic organic scales of three categories, an underlayer of 24 rows of minute more or less pentagonal scales,

into which insert two opposite rows of hair-like scales. The underlayer scales covered by 11 rows of limuloid scales. The cell body covered with organic scales arranged in two or more layers.

With the single order Pyramimonadales.

With two extant families: Pyramimonadaceae Korshikov (1938) and Halosphaeraceae Haeckel (1894).

All genera described more than a century ago: *Cymbomonas* Schiller 1913, *Pyramimonas* Schmarda (1850), *Halosphaera* Schmitz (1878), *Pterosperma* Pouchet (1893), *Pachysphaera* Ostenfeld (1899). The genus '*Prasinopapilla*' not yet formally described.

Four families of fossil genera (Tappan, 1980), comprising ~57 genera, and many additional names are considered to be synonyms. From Precambrian to Holocene. The fossil genus *Tasmanites* resembles the extant genus *Pachysphaera*, and has even been considered to be identical (Boalch & Guy-Ohlson, 1992).

Acknowledgements

We thank Dr Tatiana Yu Orlova for providing the material studied here. Lis Munk Frederiksen kindly sectioned the material used for transmission electron microscopy. Thanks to Nadezhda Rimskaya-Korsakova for her assistance in finding seawater temperatures near Vladivostok.

Disclosure statement

No potential conflict of interest was reported by the authors.

Funding

This study was supported by the Villum Kann Rasmussen Foundation (grant number not available) and Brødrene Hartmann Fonden (R69-A22.920) to ND.

Supplementary information

The following supplementary material is accessible via the Supplementary Content tab on the article's online page at <https://doi.org/10.1080/09670262.2019.1638524>

Supplementary fig. S1. Number of species of *Pyramimonas* described on a decadal basis since the description of the type species in 1850.

Author contributions

N. Daugbjerg: original concept, LM, TEM, all molecular work, figures, and writing the manuscript; N.M.D Fassel: LM, TEM, molecular laboratory work; Ø. Moestrup: received the culture, original concept, TEM and writing the manuscript.

ORCID

Niels Daugbjerg  <http://orcid.org/0000-0002-0397-3073>
Øjvind Moestrup  <http://orcid.org/0000-0003-0965-8645>

References

- Aken, M.E. & Pienaar, R.N. (1981). Observations on the reproduction of *Pyramimonas parkeae* Norris et Pearson (Prasinophyceae). *South African Journal of Science*, **77**: 330–331.
- Andersen, R.A., Berges, J.A., Harrison, P.J. & Watanabe, M. M. (2005). Recipes for freshwater and seawater media. In *Algal Culturing Techniques* (Andersen, R.A., editor), 429–538. Elsevier, Burlington, USA.
- Bhuiyan, M.A.H., Faria, D.G., Horiguchi, T., Sym, S.D. & Suda, S. (2015). Taxonomy and phylogeny of *Pyramimonas vacuolata* sp. nov. (Pyramimonadales, Chlorophyta). *Phycologia*, **54**: 323–332.
- Boalch, G.T. & Guy-Ohlson, D. (1992). *Tasmanites*, the correct name for *Pachysphaera* (Prasinophyceae, Pterospermatocataceae). *Taxon*, **41**: 529–531.
- Cavalier-Smith, T. (1993). The origins, losses and gains of chloroplasts. In *Origins of Plastids* (Lewin R.A., editor), 291–348. Chapman & Hall, New York.
- Christensen, T. (1980–1994). *Algae: A Taxonomic Survey*. AiO Print, Odense.
- Darriba, D., Taboada, G.L., Doallo, R. & Posada, D. (2012). Jmodeltest 2: more models, new heuristics and parallel computing. *Nature Methods*, **9**: 772.
- Daugbjerg, N. (2000). *Pyramimonas tychotreta* sp. nov. (Prasinophyceae), a new marine species from Antarctica: light and electron microscopy of the motile stage and notes on growth rates. *Journal of Phycology*, **36**: 160–171.
- Daugbjerg, N., Marchant, H.J. & Thomsen, H.A. (2000). Life history stages of *Pyramimonas tychotreta* (Prasinophyceae, Chlorophyta), a marine flagellate from the Ross Sea, Antarctica. *Phycological Research*, **48**: 199–209.
- Daugbjerg, N. & Moestrup, Ø. (1992a). Ultrastructure of *Pyramimonas cyrtoptera* sp. nov. (Prasinophyceae), a sixteen-flagellate species from Northern Foxe Basin, Arctic Canada, including observations on growth rates. *Canadian Journal of Botany*, **70**: 1259–1273.
- Daugbjerg, N. & Moestrup, Ø. (1992b). Fine structure of *Pyramimonas cycloretta* sp. nov. (Prasinophyceae) from Northern Foxe Basin, Arctic Canada, with some observations on growth rates. *European Journal of Protistology*, **28**: 288–298.
- Daugbjerg, N., Moestrup, Ø. & Actander, P. (1994). Phylogeny of the genus *Pyramimonas* (Prasinophyceae, Chlorophyta) inferred from the *rbcL* gene. *Journal of Phycology*, **30**: 991–999.
- Dos Santos, A.L., Pollina, T., Gourvil, P., Corre, E., Marie, D., Garrido, J.L., Rodriguez, F., Noël, M.-H., Vaultot, D. & Eikrem, W. (2017). Chloropicophyceae, a new class of picoplanktonic prasinophytes. *Scientific Reports*, **7**: 14019.
- Ettl, H. & Moestrup, Ø. (1980). Light and electron microscopical studies on *Hafniomonas* gen. nov. (Chlorophyceae, Volvocales), a genus resembling *Pyramimonas*. *Plant Systematics and Evolution*, **135**: 177–210.
- Gradinger, R. (1993). Occurrence of an algal bloom under arctic pack ice. *Marine Ecology Progress Series*, **131**: 301–305.
- Griffiths, B.M. (1909). On two new members of the Volvocaceae. *New Phytologist*, **8**: 130–137.
- Guindon, S., Dufayard, J.F., Lefort, V., Anisimova, M., Hordijk, W. & Gascuel, O. (2010). New algorithms and methods to estimate maximum-likelihood phylogenies: assessing the performance of phyml 3.0. *Systematic Biology*, **59**: 307–321.
- Guiry, M.D. & Guiry, G.M. (2019). *AlgaeBase*. World-wide electronic publication, National University of Ireland, Galway. <http://www.algaebase.org>; searched on 08 March 2019.

- Haeckel, E. (1894). *Systematische Phylogenie der Protisten und Pflanzen. Erster Theil des Entwurfs einer systematischen Stammesgeschichte*. Verlag von Georg Reimer, Berlin.
- Hansen, G., Daugbjerg, N. & Moestrup, Ø. (2018). The rock-pool dinoflagellate *Nottbeckia ochracea* gen. et comb. nov. (syn.: *Hemidinium ochraceum*) – a fine-structural and molecular study with particular emphasis on the motile stage. *Protist*, **169**: 280–306.
- Harðardóttir, S., Lundholm, N., Moestrup, Ø. & Nielsen, T. G. (2014). Description of *Pyramimonas diskoicola* sp. nov. and the importance of the flagellate *Pyramimonas* (Prasinophyceae) in Greenland Sea ice during the winter–spring transition. *Polar Biology*, **37**: 1479–1484.
- Hasegawa, T., Miyashita, H., Kawachi, M., Ikemoto, H., Kurano, N., Miyachi, S. & Chihara, M. (1996). *Prasinoderma coloniale* gen. et sp. nov., a new pelagic coccoid prasinophyte from the western Pacific Ocean. *Phycologia*, **35**: 170–176.
- Hodgetts, W.J. (1920). Notes on freshwater algae. I–IV. *New Phytologist*, **19**: 254–263.
- Hori, T., Moestrup, Ø. & Hoffman, L.R. (1995). Fine structural studies on an ultraplanktonic species of *Pyramimonas*, *P. virginica* (Prasinophyceae), with a discussion of subgenera within the genus *Pyramimonas*. *European Journal of Phycology*, **30**: 219–234.
- Inouye, I., Hori, T. & Chihara, M. (1985). Ultrastructural characters of *Pyramimonas* (Prasinophyceae) and their possible relevance in taxonomy. In *Origin and Evolution of Diversity in Plants and Plant Communities* (Hara, H., editor), 314–327. Academia Scientific Book Inc., Tokyo.
- Korshikov, O.A. (1938). Volvocineae. In *Vyznachnykh vodorostej URSS, IV*. Akademie Nauk URSS, Kiev 184 pp.
- Kumar, S., Stecher, G., Li, M., Nnyaz, C. & Tamura, K. (2018). MEGA X: Molecular evolutionary genetics analysis across computing platforms. *Molecular Biology and Evolution*, **35**: 1547–1549.
- Larkin, M.A., Blackshields, N.P., Brown, N.P., Chenna, R., McGettigan, P.A., McWilliam, H., Valentin, F., Wallace, I.M., Wilm, A., Lopez, R., Thompson, J.D., Gibson, T.J. & Higgins, D.G. (2007). Clustal W and Clustal X version 2.0. *Bioinformatics*, **23**: 2947–2948.
- Leliaert, F., Tronholm, A., Lemieux, C., Turmel, M., DePriest, M.S., Bhattacharya, D., Karol, K.G., Fredericq, S., Zechman, F.W. & Lopez-Bautista, J.M. (2016). Chloroplast phylogenomic analyses reveal the deepest-branching lineage of the Chlorophyta, Palmophyllophyceae class. nov. *Scientific Reports*, **6**: 25367.
- Marin, B. & Melkonian, M. (1999). Mesostigmatophyceae, a new class of streptophyte green algae revealed by SSU rRNA sequence comparisons. *Protist*, **150**: 399–417.
- Marin, B. & Melkonian, M. (2010). Molecular phylogeny and classification of the Mamiellophyceae class. nov. (Chlorophyta) based on sequence comparisons of the nuclear- and plastid-encoded rRNA operons. *Protist*, **161**: 304–336.
- Massjuk, N.P. (2006). Chlorodendrophyceae class. nov. (Chlorophyta, Viridiplantae) in the Ukrainian flora. I. The volume, phylogenetic relations and taxonomical status. *Ukrainian Botanical Journal*, **63**: 601–614 (in Ukrainian with English abstract and English diagnosis).
- McFadden, G.I., Hill, D.R.A. & Wetherbee, R. (1986). A study of the genus *Pyramimonas* from southeastern Australia. *Nordic Journal of Botany*, **6**: 209–234.
- McFadden, G.I., Hill, D.R.A. & Wetherbee, R. (1987). Electron microscopic observations on *Pyramimonas olivacea* N. Carter (Prasinophyceae, Chlorophyta). *Phycologia*, **26**: 322–327.
- Moestrup, Ø. & Thomsen, H.A. (1980). Preparation of shadow-cast whole mounts. In *Handbook of Phycological Methods: Developmental and Cytological Methods* (Stein-Taylor, J.R. & Gantt, E., editors), 385–390. Cambridge: Cambridge University Press.
- Moestrup, Ø., & Hill, D.R.A. (1991). Studies on the genus *Pyramimonas* (Prasinophyceae) from Australian and European waters. *P. propulsa* sp. nov. and *P. mitra* sp. nov. *Phycologia*, **30**: 534–546.
- Moestrup, Ø. & Hill, D.R.A. (1993). Reconstruction of the flagellar surface armour in *Pyramimonas mantoniae* sp. nov. and *Pyramimonas mitra* Moestrup & Hill (Prasinophyceae). *Phycologia*, **32**: 59–67.
- Moestrup, Ø., Inouye, I. & Hori, T. (2003). Ultrastructural studies on *Cymbomonas tetramitiformis*. I. (Prasinophyceae). General structure, scale microstructure and ontogeny. *Canadian Journal of Botany*, **81**: 657–671.
- Moestrup, Ø. & Thomsen, H.A. (1974). An ultrastructural study of the flagellate *Pyramimonas orientalis* with particular emphasis on Golgi apparatus activity and the flagellar apparatus. *Protoplasma*, **81**: 247–269.
- Moro, I., La Rocca, N., Valle, L.D., Moschin, E., Negrisolo, E. & Andreoli, C. (2002). *Pyramimonas australis* sp. nov. (Prasinophyceae, Chlorophyta) from Antarctica: fine structure and molecular phylogeny. *European Journal of Phycology*, **37**: 103–114.
- Nakayama, T., Suda, S., Kawachi, M. & Inouye, I. (2007). Phylogeny and ultrastructure of *Nephroselmis* and *Pseudoscourfieldia* (Chlorophyta), including the description of *Nephroselmis anterostigmatica* sp. nov. and a proposal for the Nephroselmiales ord. nov. *Phycologia*, **46**: 680–697.
- Orlova, T.Y., Stonik, V. & Shevchenko, O.G. (2009). Flora of planktonic microalgae of Amursky Bay, Sea of Japan. *Russian Journal of Marine Biology*, **35**: 60–78.
- Ostenfeld, C.H. (1899). In *Iagttagelser over overfladevandets temperatur, saltholdighed og plankton på islandske og grønlandske skibsrouter i 1898* (Knudsen, M. & Ostenfeld, C.H., editors). Bianco Lunos Kgl. Hof-Bogtrykkeri (F. Dreyer), Kjøbenhavn, 93 pp.
- Parke, M. & Hartog-Adams, I den (1965). Three species of *Halosphaera*. *Journal of the Marine Biological Association of the United Kingdom*, **45**: 537–557.
- Ponomarenko, L.P., Stonik, I.V., Aizdaicher, N.A., Orlova, T.Y., Popovskaya, G.V., Pomaskina, G.V. & Stonik, V.A. (2004). Sterols of marine microalgae *Pyramimonas* cf. *cordata* (Prasinophyta), *Attheya ussurenensis* sp. nov. (Bacillariophyta) and a spring diatom bloom from Lake Baikal. *Comparative Biochemistry and Physiology Part B*, **138**: 65–70.
- Pouchet, G. (1893). Histoire naturelle. In *Voyage de La Manche à l'Île Jan Mayen et au Spitzberg (Juillet–Août 1892)*. *Nouvelles Archives des Missions Scientifiques et Littéraires*, **5**: 155–217.
- Ronquist, F. & Huelsenbeck, J.P. (2003). MrBayes 3: Bayesian phylogenetic inference under mixed models. *Bioinformatics*, **19**: 1572–1574.
- Round, F.E. (1971). The taxonomy of the Chlorophyta. II. *British Phycological Journal*, **6**: 235–264.
- Schiller, J. (1913). Vorläufige Ergebnisse der Phytoplankton-untersuchungen auf den Fahrten S.M.S. “Najade” in der Adria. II Flagellaten und Chlorophyceen. *Sitzungsberichte der Kaiserlichen Akademie der Wissenschaften in Wien. Mathematisch-naturwissenschaftliche Klasse*, **122**: 1–10.

- Schmarda, L.K. (1850). Neue Formen von Infusorien. Denkschriften der Kaiserlichen Akademie der Wissenschaften, Wien. *Mathematisch-Naturwissenschaftliche Klasse*, **1**: 9–14.
- Schmitz, F. (1878). *Halosphaera*, eine neue Gattung grüner Algen aus dem Mittelmeer. *Mittheilungen aus dem Zoologischen Station zu Neapel*, **1**: 68–92.
- Stonik, I.V. & Aizdaicher, N.A. (2005). Studies on morphology of species from the genus *Pyramimonas* Schmarda (Prasinophyceae) new for the Far Eastern seas of Russia. *International Journal on Algae*, **7**: 247–255.
- Suda, S., Bhuiyan, M.A.H. & Faria, D.G. (2013). Genetic diversity of *Pyramimonas* from Ryukyu Archipelago, Japan (Chlorophyceae, Pyramimonadales). *Journal of Marine Science and Technology*, **21**: 285–296.
- Sym, S.D. & Pienaar, R.N. (1997). Further observations on the type subgenus of *Pyramimonas* (Prasinophyceae), with particular reference to a new species, *P. chlorina*, and the flagellar apparatus of *P. propulsa*. *Canadian Journal of Botany*, **75**: 2196–2215.
- Tappan, H. (1980). *The Palaeobiology of Plant Protists*. W. H. Freeman and Co., San Francisco.
- Thomsen, H.A. (1982). Planktonic choanoflagellates from Disko Bugt, West Greenland, with a survey of the marine nanoplankton of the area. *Meddelelser om Grønland, Bioscience*, **8**: 3–35.
- Thomsen, H.A. (1988). Fine structure of *Pyramimonas nansenii* (Prasinophyceae) from Danish coastal waters. *Nordic Journal of Botany*, **8**: 305–318.
- Thronsdon, J. & Moestrup, Ø. (1988). Light and electron microscopical studies on *Pseudoscourfieldia marina*, a primitive scaly green flagellate (Prasinophyceae) with posterior flagella. *Canadian Journal of Botany*, **66**: 1415–1434.
- Tragin, M. & Vault, D. (2018). Green microalgae in marine coastal waters: The Ocean Sampling Day (OSD) dataset. *Scientific Reports*, **8**: 14020.
- Tragin, M., Zingone, A. & Vault, D. (2018). Comparison of coastal phytoplankton composition estimated from the V4 and V9 regions of the 18S rRNA gene with a focus on photosynthetic groups and especially Chlorophyta. *Environmental Microbiology*, **20**: 506–520.
- Van den Hoff, J., Burton, H.R. & Vest, M. (1989). An encystment stage, bearing a new scale type, of the Antarctic prasinophyte *Pyramimonas gelidicola* and its paleolimnological and taxonomic significance. *Journal of Phycology*, **25**: 446–454.
- Van Den Hoff, J. & Ferris, J.M. (2009). Pleomorphism in the Antarctic flagellate *Pyramimonas gelidicola* (Prasinophyceae, Chlorophyta). *Polar Research*, **28**: 426–432.
- Waterhouse, A.M., Procter, J.B., Martin, D.M.A., Clamp, M. & Barton, G.J. (2009). Jalview version 2 - a multiple sequence alignment editor and analysis workbench. *Bioinformatics*, **25**: 1189–1191.